Composites: Part A xxx (2015) xxx–xxx

Contents lists available at ScienceDirect

Composites: Part A

journal homepage: www.elsevier.com/locate/compositesa

Retention of mechanical performance of polymer matrix composites above the glass transition temperature by vascular cooling

Anthony M. Coppola [a,c], Anthony S. Griffin [b,c], Nancy R. Sottos [b,c], Scott R. White [a,c,*]

[a] Department of Aerospace Engineering, University of Illinois at Urbana-Champaign, Urbana, IL 61801, USA
[b] Department of Material Science and Engineering, University of Illinois at Urbana-Champaign, Urbana, IL 61801, USA
[c] Beckman Institute for Advanced Science and Technology, University of Illinois at Urbana-Champaign, Urbana, IL 61801, USA

ARTICLE INFO

Article history:
Received 16 March 2015
Received in revised form 14 July 2015
Accepted 18 July 2015
Available online xxxx

Keywords:
B. Thermomechanical
B. High-temperature properties
Vascular cooling

ABSTRACT

An actively cooled vascular polymer matrix composite containing 3.0% channel volume fraction retains greater than 90% flexural stiffness when exposed continuously to 325 °C environmental temperature. Non-cooled controls suffered complete structural failure through thermal degradation under the same conditions. Glass–epoxy composites (T_g = 152 °C) manufactured by vacuum assisted resin transfer molding contain microchannel networks of two different architectures optimized for thermal and mechanical performance. Microchannels are fabricated by vaporization of poly(lactide) fibers treated with tin(II) oxalate catalyst that are incorporated into the fiber preform prior to resin infiltration. Flexural modulus, material temperature, and heat removal rates are measured during four-point bending testing as a function of environmental temperature and coolant flow rate. Simulations validate experimental measurements and provide insight into the thermal behavior. Vascular specimens with only 1.5% channel volume fraction centered at the neutral bending axis also retained over 80% flexural stiffness at 325 °C environmental temperature.

1. Introduction

Polymer matrix composites (PMCs) are susceptible to reduced structural performance at elevated temperatures, such as those experienced during high speed flight [1–3], vehicle transportation [4–6], and during cycling of batteries, fuel cells, and other electronics [7–9]. Typical polymer matrices, such as epoxy, polyester, and vinyl-ester, have glass transition temperatures (T_g) at or below 200 °C, forcing the use of alternative materials such as metals and ceramics at service temperatures [3]. Subjecting a composite to high temperature, even for short time periods, can cause permanent damage, including delamination, matrix cracking, plastic deformation, and ultimately combustion and fire [10–13]. As an alternative, circulation of coolant through microvascular channels embedded directly into the PMC can regulate temperature by removing heat [14–16], potentially enabling safe structural performance under high thermomechanical loading.

In PMCs, vascular networks have been fabricated by solder removal [17,18], manual extraction of a solid wire [19–21], integration of hollow tubules or fibers [22–28], and Vaporization of Sacrificial Components (VaSC) [29–31]. Unlike most other methods which are restricted to straight channels with one-dimensional connectivity, VaSC using sacrificial fibers (SF) allows for three-dimensional, interconnected vascular architectures. To create a hollow channel poly(lactic acid) (PLA) SFs are integrated into textile weaving or braiding operations, survive standard composite manufacturing processing, and then are subsequently removed during a 200 °C post-cure [30]. When manufactured to minimize distortions to the structural fiber architecture, channels had minimal effect on tensile and compressive strength and modulus [21,26,31], interlaminar fracture toughness [19,25,27], and impact resistance [17,18,24,28].

Kozola et al. [14] studied active cooling in a vascularized epoxy fin heated at the base and reported up to a 53-fold increase in the effective heat transfer coefficient compared to an uncooled fin, while reducing the mean field temperature from 60 °C to 30 °C. Soghrati et al. [15,16] computationally modeled active cooling in 3D woven microvascular composites subjected to constant heat flux on one surface. Design charts related the maximum allowable temperature to the coolant flow rate and delivered heat flux. Phillips et al. [25] evaluated thermal transport in an actively heated carbon/epoxy fin subject to free convective cooling using

* Corresponding author at: 306 Talbot Laboratory, 104 South Wright Street, Urbana, IL 61801, USA. Tel.: +1 217 333 1077.
E-mail address: swhite@illinois.edu (S.R. White).

http://dx.doi.org/10.1016/j.compositesa.2015.07.012
1359-835X/

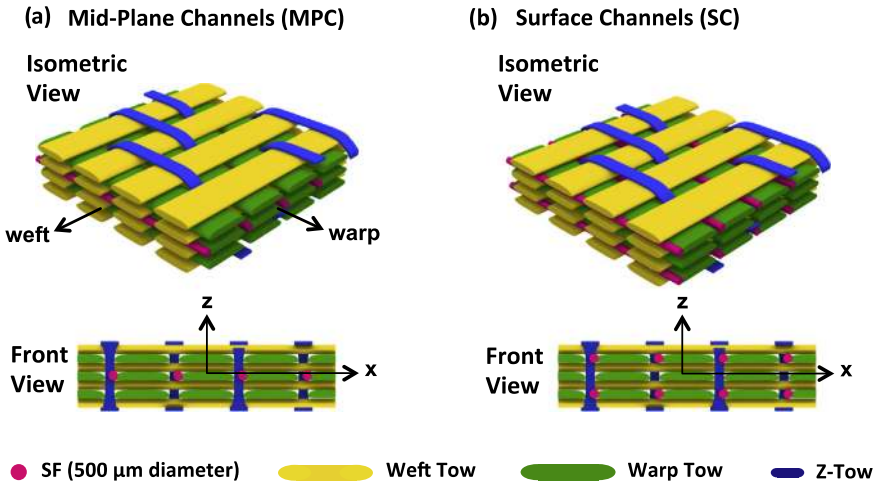

Fig. 1. Vascular composite specimens and channel architectures. The textile is composed of 3 warp layers and 4 weft layers, which are held together by the *z*-fibers. The areal density of the fabric is 4.07 kg/m^2 (120 oz/yard^2). In the warp layers there are 3.0 tows/cm and in the weft layers there are 2.7 tows/cm. The fiber content in the *x* and *y* directions are nearly equivalent as a result of the difference in tow density. (a) Mid-plane channel (MPC) architecture contains four channels located at the mid-plane of the sample yielding a total channel volume fraction of V_c = 1.5%. (b) Surface channel (SC) architecture contains four channels located at each surface of the sample yielding a total channel volume fraction of V_c = 3.0%. (For interpretation of the references to color in this figure legend, the reader is referred to the web version of this article.)

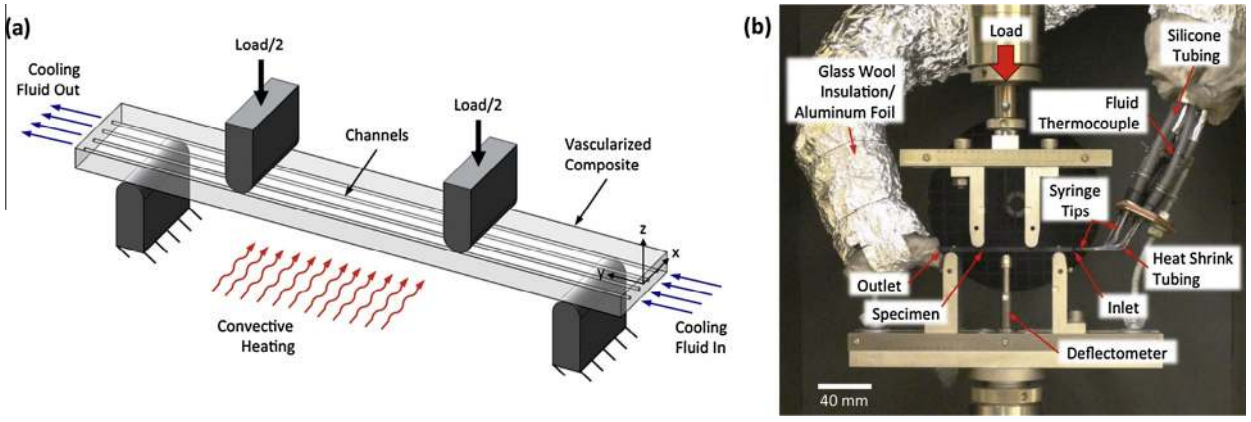

Fig. 2. Active cooling test set-up. (a) Schematic of active cooling test concept. Heat is removed by coolant pumped through the channels at a constant rate, reducing the temperature of the composite and improving mechanical properties. Heat is supplied convectively by the environmental chamber and conductively by the test fixtures. A coordinate axis is included for reference, with the origin centered on the inlet face. (b) Photograph of the test setup inside the environmental chamber showing the placement of the specimen, test fixture, and the coolant delivery system. (For interpretation of the references to color in this figure legend, the reader is referred to the web version of this article.)

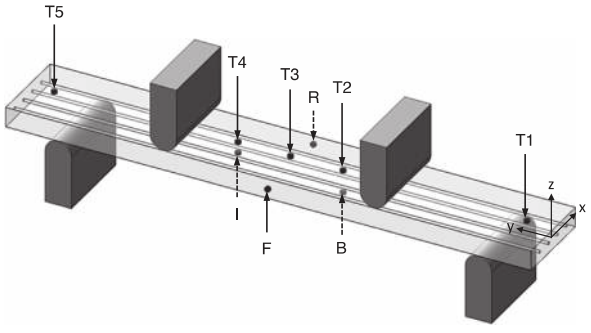

Fig. 3. Thermocouple locations in actively cooled composites. Top surface thermocouples (T1-5) were placed at (*x*, *y*, *z*) = (0, *y*, 1.75) where *y* = 5, 40, 50, 60, and 95. One each was placed on the front (F) and rear (R) edge of the specimen at (*x*, *y*, *z*) = (±8, 50, 0). One thermocouple was placed inside (I) of the specimen at (*x*, *y*, *z*) = (0, 60, 0) to measure the internal temperature and one on the bottom (B) surface at (*x*, *y*, *z*) = (0, 40, −1.75). Dashed lines indicate thermocouples that are not located on the visible surface in the given view. Dimensions are in mm.

thermography to measure surface temperature. In a related study, Phillips and Baur [32] studied activation and deactivation of a shape memory polymer using microvascular heating and cooling, respectively. The authors developed a non-dimensional analytical model to analyze and predict the heat transfer and temperature fields. None of these prior studies have examined thermomechanical performance during active cooling.

In this study we demonstrate the effectiveness of active cooling through a vascularized composite to reduce temperature and maintain structural performance while subject to a convective environment at temperatures greater than T_g. Flexural testing of vascular specimens in an environmentally controlled chamber was carried out. The vascular composite is composed of a three-dimensional orthogonally woven glass fiber textile infused with epoxy and vascularized using VaSC. Composites containing channels at the mid-plane (i.e. *mid-plane channels* – "MPC") and those containing channels at the surfaces (*i.e. surface channels* – "SC") are compared. Both architectures were tested with active cooling using water for a variety of flow rates in the laminar regime

Please cite this article in press as: Coppola AM et al. Retention of mechanical performance of polymer matrix composites above the glass transition temperature by vascular cooling. Composites: Part A (2015), http://dx.doi.org/10.1016/j.compositesa.2015.07.012

Table 1
Channel flow rate, total flow rate and Reynolds number for MPC and SC specimens.

	Channel flow rate (mL/min)			
	5	10	20	40
Mid-plane cooled (4 channels)				
Total flow rate	20	40	80	160
Reynolds number[a]	242–653	451–842	864–1249	1687–2102
Surface cooled (8 channels)				
Total flow rate	40	80	160	320
Reynolds number[a]	246–546	450–743	844–1148	1629–1987

[a] Reynolds number range calculated using Eq. (6) based on the coolant temperature at the inlet and outlet.

and environmental temperatures up to 325 °C. Simulations are used to validate experimental measurements and gain further insight into the relationship between active cooling parameters and temperature field.

2. Material preparation procedures

2.1. Sacrificial fiber synthesis

Sacrificial fibers for the VaSC process were prepared from 500 μm diameter PLA monofilament fiber (Nextrusion Inc.) treated with tin(II) oxalate (SnOx) catalyst using a modified procedure first outlined by Esser-Kahn et al. [30] and Dong et al. [29]. The as-received fiber was wound on a custom reel and placed in a 1000 mL treatment bath composed of 480 mL trifluoroethanol (TFE, Sigma–Aldrich), 320 mL deionized water, 13 g SnOx (Sigma–Aldrich), 40 mL Disperbyk 187 surfactant (BYK Chemie), and 1 g Rhodamine 6G dye (Sigma–Aldrich). To ensure a neutral pH, 20% aqueous sodium hydroxide was added to the bath until a pH between 6.8 and 7.2 was achieved. The fiber reel was spun in solution at 400–450 rpm for 24 h at 37 °C, then removed and allowed to dry for 24 h at 35 °C in a convection oven.

2.2. Composite specimen manufacture

Composite specimens were manufactured from a three-dimensional orthogonally woven S2 glass fiber textile with an areal density of 4.07 kg/m^2 (TEAM Inc.), shown schematically in Fig. 1. The SFs were positioned in the textile by hand using a sewing needle. Resin was infused into the glass/SF preform using a double bag vacuum assisted resin transfer molding (VARTM) technique. EPON 862 resin (Miller–Stephenson) and EPIKURE W curing agent (Miller–Stephenson) were mixed in a ratio of 100:26.4 by mass and degassed at 70 °C for 2–3 h. During this time the layup was pre-heated to 100 °C in a convection oven to facilitate a warm infusion, reducing viscosity and aiding infiltration. Following infusion, the vacuum line to the inner bag was closed off and the layup was heated at 3 °C/min to 121 °C and cured for 8 h before cooling down at 1 °C/min to room temperature. Sacrificial components were removed from the composites using a VaSC treatment at 200 °C under vacuum for 24 h. The post-cure caused slight browning of the matrix material which was attributed to mild oxidation of the resin. The composites had an average fiber volume of 44.5 ± 1.3% as measured by matrix burn-off. The thickness of the final composites ranged from 3.5 to 3.8 mm.

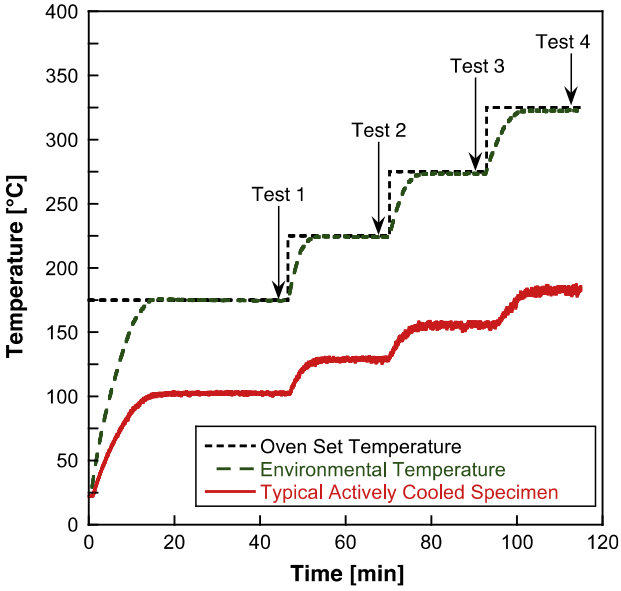

Fig. 4. Typical temperature profiles for thermomechanical testing of actively cooled specimens, which were tested at four different environmental temperatures in succession. The oven set temperature, the actual environmental temperature, and the surface temperature of a typical actively cooled specimen are compared, showing the time required to reach steady state. Actual environmental chamber temperature was measured by an E-type thermocouple suspended near the test region. Actively cooled specimen temperature was measured by an E-type thermocouple touching the specimen surface. (For interpretation of the references to color in this figure legend, the reader is referred to the web version of this article.)

Composites panels were cut to approximate size using a water cooled diamond saw and finished to 100 mm × 16 mm specimens using an end-mill, with the warp direction positioned along the long (y) axis. Prior to testing, all composites were coated with high temperature black paint (Zynolyte Z635) to ensure uniform emissivity of the surface.

Three types of specimens were manufactured: those containing channels at the mid-plane (MPC, Fig. 1a), those containing channels near the top and bottom surfaces (SC, Fig. 1b), and control specimens with no channels. Specimens containing no channels were used as non-cooled controls. MPC specimens were designed to maximize flexural modulus by placing the channels at the neutral axis of the specimen. SC specimens were designed to maximize cooling effectiveness by placing the channels near the boundaries of the composite and distributing the flow through more channels.

2.3. Neat epoxy specimen manufacture

Epoxy sheets were made for thermomechanical analysis of the matrix material using EPON 862 resin (Miller–Stephenson) and EPIKURE W curing agent (Miller–Stephenson), mixed in a ratio of 100:26.4 by mass. The epoxy was degassed at 70 °C for up to 3 h,

Table 2
Average composite temperature and average coolant outlet temperature as a function of total number of elements for the MPC sample simulations. The ratio of solid to fluid elements was held constant.

Number of elements	Average coolant outlet temperature (°C)	Average composite temperature (°C)
84,000	28.67	152.95
250,200	28.67	153.05
517,050	28.65	153.39

Table 3
Flexural modulus at room temperature for control and vascularized composites. Error bounds represent one standard deviation based on the results of eight tests.

Sample type	Number of samples tested	Flexural modulus (GPa)
Controls (no channels)	8	17.1 ± 0.35
MPC (mid-plane channels)	8	17.0 ± 0.52
SC (surface channels)	8	16.5 ± 0.43

Please cite this article in press as: Coppola AM et al. Retention of mechanical performance of polymer matrix composites above the glass transition temperature by vascular cooling. Composites: Part A (2015), http://dx.doi.org/10.1016/j.compositesa.2015.07.012

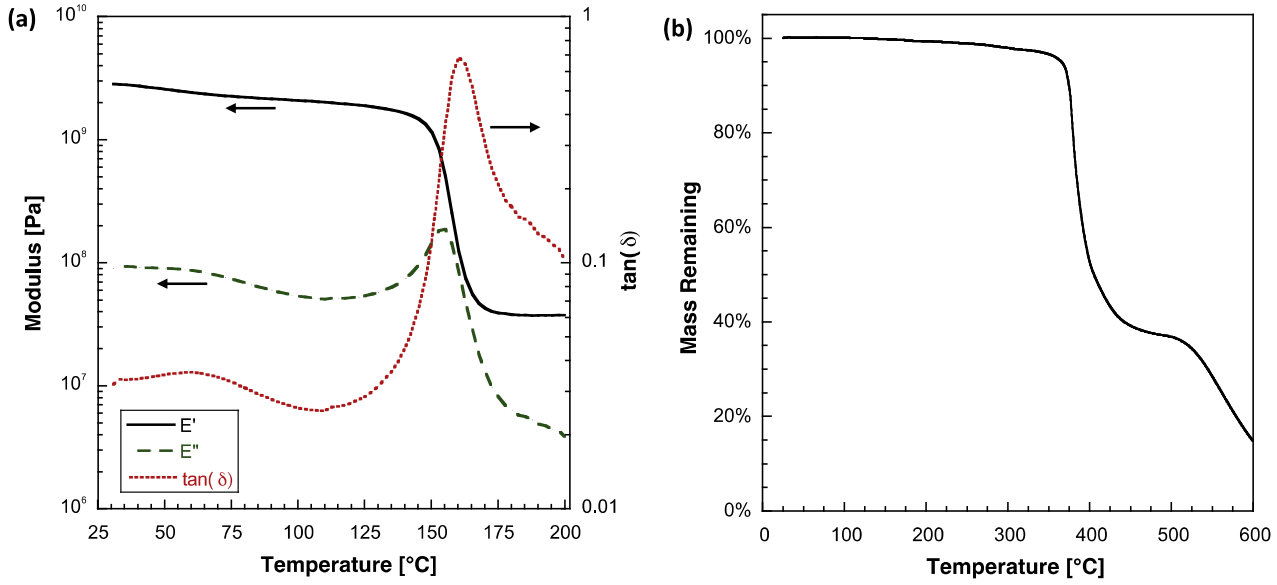

Fig. 5. Thermal and mechanical characterization of the epoxy matrix. (a) DMA testing results showing the storage modulus (E'), the loss modulus (E'') and tan(δ). (b) TGA testing results in an air/nitrogen environment (flow rates of 35 mL/min for each). (For interpretation of the references to color in this figure legend, the reader is referred to the web version of this article.)

then poured into a 2 mm thick closed mold and cured at 121 °C for 8 h with 3 °C/min heating and cooling rates. To replicate the processing conditions for the vascularized composites, the epoxy was then placed in a vacuum oven for 24 h at 200 °C.

3. Testing and analysis procedures

3.1. Characterization of actively cooled composites

3.1.1. Test setup

Mechanical performance of the active cooled specimens was evaluated using a four-point bend test inside an environmental chamber while coolant was circulated through the specimen (Fig. 2). A flexural test was chosen primarily because it allowed for simple attachment of the coolant delivery system to the specimen. All testing was performed on an electromechanical testing frame (Instron, Model 5984) equipped with a four-point bending fixture (Instron, Model 2810-400). Load was measured using a 5 kN load cell (Instron, Model 2580), and strain was measured from center point deflection using a video extensometer (Instron, Model 2663-821) with a 60 mm field of view. Heat was delivered by an environmental chamber (Instron, Model 3119-410), which provided convectively heated airflow, as well as conduction from contact with the bending fixture.

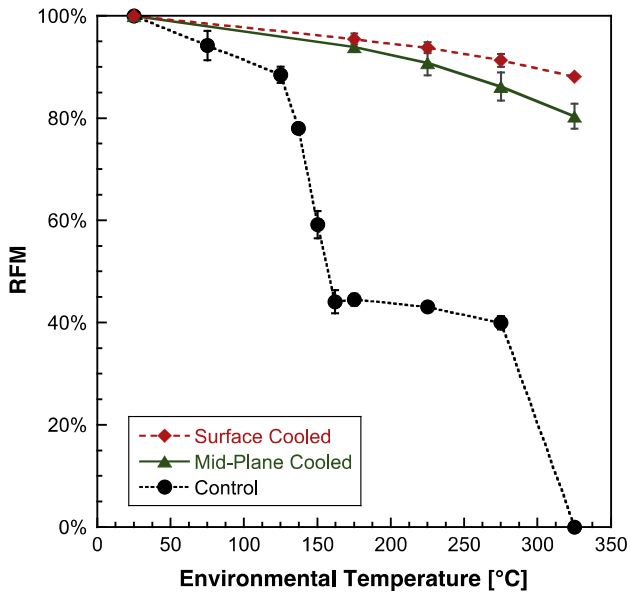

Fig. 6. Retained flexural modulus (RFM) as a function of environmental temperature. Control specimens (no microchannels) were thermally degraded at 325 °C and retained no flexural capacity. Vascular specimens were tested with a coolant flow rate of 160 mL/min. Error bars represent one standard deviation. (For interpretation of the references to color in this figure legend, the reader is referred to the web version of this article.)

Coolant was pumped through each channel independently in actively cooled specimens using a peristaltic pump (Cole–Parmer, Model EW-07551-00), ensuring equal flow in each channel. Tap water stored at room temperature was used as coolant and was not recirculated to ensure constant supply temperature. Fluid was delivered via 1/4 in. OD, 1/8 in. ID silicone rubber tubing connected to the channels using 21 gage stainless steel syringe tips linked by low contraction, high temperature heat shrink tubing (fluorinated ethylene propylene). One syringe tip was connected to the silicone tubing, while the other was inserted 2–3 mm into a hole drilled in the end of the channel and sealed with epoxy adhesive (J-B Weld epoxy). The heat shrink tubing was sufficiently flexible to prevent mechanically constraining the specimen motion during testing. The delivery setup was insulated with glass wool wrapped in aluminum foil to minimize heating of the fluid prior to delivery into the specimen.

The fluid temperature was measured near the inlet and outlet of the specimen using type T thermocouples (Omega Engineering, Model TMQSS-020U) inserted into 4 of the 8 tubing connections. All four channels were monitored for the MPC specimens and the top four in the SC specimens (which were independently verified to provide similar data to the bottom four channels). Thermocouples were inserted into a hole drilled in a 1/8″ straight barbed polycarbonate fitting and positioned in the middle of the flow path then sealed with epoxy adhesive. Thermocouple data was collected using several four-input temperature sensors (Phidgets, Model 1048) and recorded using a custom LabVIEW code (National Instruments) at 1 Hz continuously.

Specimen temperature was measured using type E thermocouples (Omega Engineering, Model EMQSS-020U) placed as shown in

Table 4
Flexural modulus results for all test conditions. Control specimens do not contain microchannels. Active cooling results are arranged by total flow rate. Error bounds represent one standard deviation.

T (Environment) (°C)	Flexural modulus (GPa)								
	Control	Mid-plane cooled (MPC) Total flow rate (mL/min)				Surface cooled (SC) Total flow rate (mL/min)			
		20	40	80	160	40	80	160	320
25	17.2 ± 0.4	17.2 ± 0.3	17.4 ± 0.4	17.2 ± 0.4	17.3 ± 0.3	17.3 ± 0.2	17.4 ± 0.2	17.1 ± 0.2	17.3 ± 0.2
75	16.2 ± 0.3	–	–	–	–	–	–	–	–
125	15.2 ± 0.4	–	–	–	–	–	–	–	–
137	13.4 ± 0.4	–	–	–	–	–	–	–	–
150	10.1 ± 0.3	–	–	–	–	–	–	–	–
162	7.70 ± 0.40	–	–	–	–	–	–	–	–
175	7.67 ± 0.17	16.1 ± 0.1	16.2 ± 0.4	16.3 ± 0.2	16.3 ± 0.2	16.3 ± 0.3	16.6 ± 0.1	16.4 ± 0.2	16.6 ± 0.2
225	7.25 ± 0.12	15.2 ± 0.2	15.6 ± 0.3	15.6 ± 0.2	15.7 ± 0.2	15.9 ± 0.6	16.0 ± 0.1	16.1 ± 0.3	16.2 ± 0.2
275	6.94 ± 0.27	13.8 ± 0.5	14.5 ± 0.2	14.8 ± 0.2	14.9 ± 0.3	15.0 ± 0.5	15.5 ± 0.1	15.7 ± 0.2	15.8 ± 0.1
325	0[a]	11.5 ± 0.3	13.0 ± 0.1	13.5 ± 0.3	13.9 ± 0.2	14.2 ± 0.6	14.8 ± 0.1	15.1 ± 0.2	15.4 ± 0.1

[a] Thermal degradation of epoxy occurred.

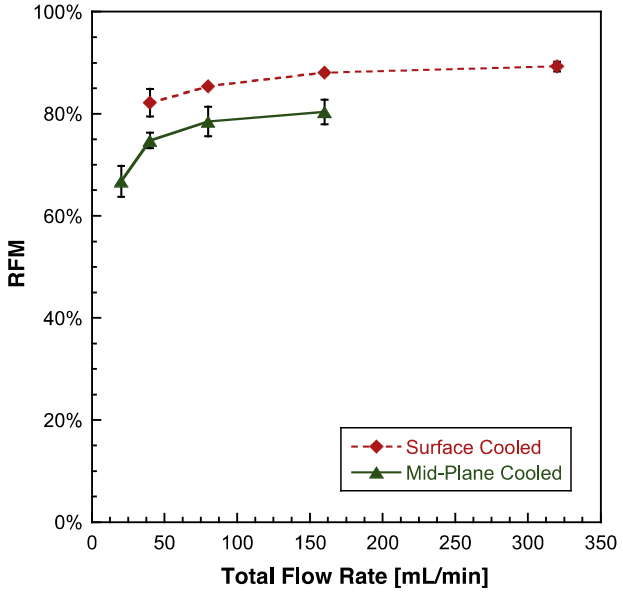

Fig. 7. RFM as a function of the total coolant flow rate in a 325 °C environment. Error bars represent one standard deviation. (For interpretation of the references to color in this figure legend, the reader is referred to the web version of this article.)

Fig. 3. Surface thermocouples were held in place using a small amount of epoxy adhesive (J-B Weld). The internal thermocouple was inserted into a small hole of the same diameter drilled into the specimen and sealed in place with epoxy. Temperature was collected using the same data acquisition method used to record fluid temperature.

3.1.2. Test procedure

Actively cooled test conditions are summarized in Table 1. MPC specimens containing 4 channels and SC specimens containing 8 channels were evaluated at flow rates of 5, 10, 20 and 40 mL/min per channel. Total flow rate for each architecture differed based on the total number of channels. The Reynolds number was <2300 for all flow rates, indicating laminar flow (see Section 3.1.3 for calculation of Reynolds number).

For thermomechanical testing, samples were evaluated in four-point bending according to ASTM D7264. The outer span was 80 mm and the inner span was 40 mm. Tests were performed at a constant displacement rate of 1 mm/min to a maximum strain of 0.21% to avoiding damage to the specimen and allow for multiple tests of the same specimen at different temperatures and flow rates. Tests were conducted at four elevated temperature conditions in succession (175 °C, 225 °C, 275 °C, and 325 °C) according to the protocol shown in Fig. 4 in order to achieve steady state conditions. Following a complete round of testing (to 325 °C) the oven was cooled naturally to room temperature and the process was repeated at the next flow rate. No deformation or changes in room temperature flexural modulus were observed in the specimens after each testing cycle. Three specimens were tested for both vascular architectures.

Separate tests were conducted for thermal characterization of the specimens using embedded thermocouples as specified in Fig. 3. The environmental temperature was again increased sequentially (175 °C, 225 °C, 275 °C, and 325 °C), but at each temperature all flow rates (5–40 mL/min) were tested to expedite testing. Results using this protocol were compared to results from the protocol used for mechanical testing, and no differences in specimen temperature were found. Again, three tests were performed for each vascular architecture.

3.1.3. Data analysis

Flexural modulus was calculated as the secant modulus from 0.1 to 0.2% maximum flexural strain. The retained flexural modulus (RFM) was calculated as

$$\mathrm{RFM} = \frac{E(T^*)}{E(T_{RT})}, \tag{1}$$

where $E(T_{RT})$ is the room temperature flexural modulus and $E(T^*)$ is the flexural modulus at T^* = environmental temperature of the chamber. Both temperatures are in °C. The total heat removal rate was calculated as

$$q = \sum_{n=4\ or\ 8} (Q\rho c_p \Delta T)_n, \tag{2}$$

where Q is the volumetric flow rate of the coolant in each channel, ρ is the density of the fluid, c_p is the specific heat capacity of the fluid, and ΔT is the change in fluid temperature from inlet to outlet for each channel. n is the number of channels and is equal to 4 for the MPC specimens and 8 for the SC specimens. Density and specific heat capacity were taken from tabulated data using average fluid temperature based on inlet and outlet fluid temperature. The total pumping power is equal to

$$P = \sum_{n=4\ or\ 8} (Q\Delta p)_n, \tag{3}$$

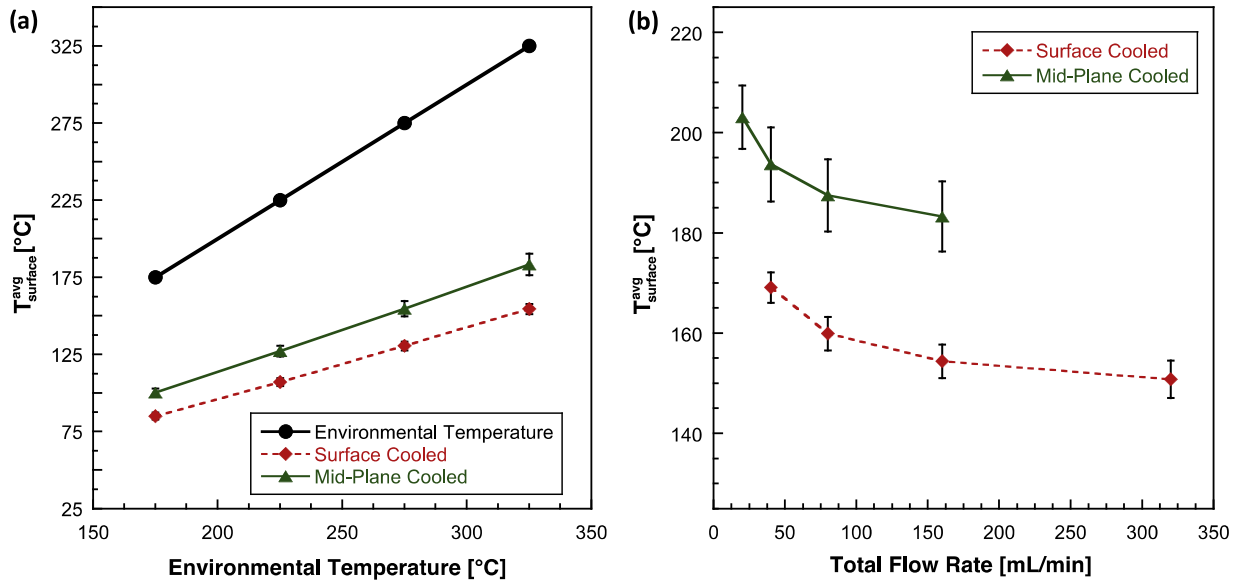

Fig. 8. Average surface temperature ($T^{avg}_{surface}$) for vascular specimens for all testing conditions. (a) Top surface temperature as a function of environmental temperature for a fixed total flow rate of 160 mL/min. (b) Top surface temperature as a function of total coolant flow rate for a fixed environmental temperature of 325 °C. Error bars represent one standard deviation. (For interpretation of the references to color in this figure legend, the reader is referred to the web version of this article.)

Table 5
Average top surface temperature for actively cooled specimens as a function of total flow rate. Error bounds represent one standard deviation.

T (Environment) (°C)	Average top surface temperature (°C)							
	Mid-plane cooled (MPC) Total flow rate (mL/min)				Surface cooled (SC) Total flow rate (mL/min)			
	20	40	80	160	40	80	160	320
175	110 ± 3	105 ± 3	102 ± 3	100 ± 3	93 ± 2	88 ± 2	85 ± 2	83 ± 2
225	140 ± 4	134 ± 4	130 ± 4	127 ± 4	117 ± 3	111 ± 3	107 ± 3	105 ± 3
275	171 ± 5	163 ± 5	158 ± 5	155 ± 5	142 ± 3	135 ± 3	130 ± 3	127 ± 3
325	203 ± 6	194 ± 7	188 ± 7	183 ± 7	169 ± 3	160 ± 3	154 ± 3	151 ± 4

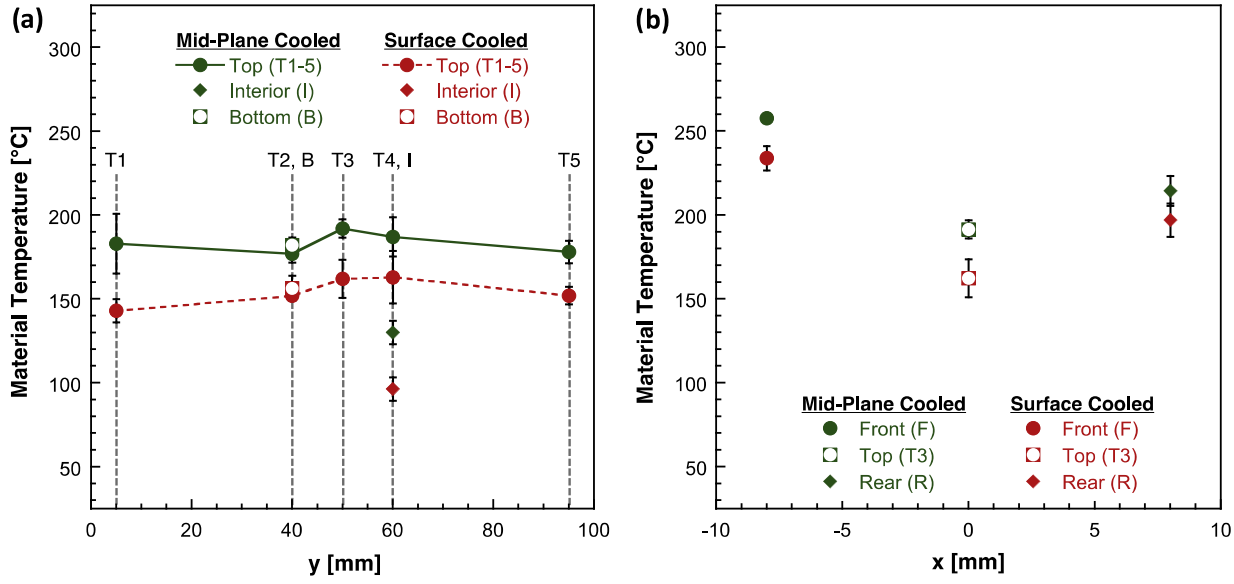

Fig. 9. Temperature distribution for actively cooled specimens. Temperature (a) along the $x = 0$ plane and (b) along the $y = 50$ mm plane for actively cooled composites in a 325 °C environment at a total flow rate of 160 mL/min. See Fig. 3 for detailed description of thermocouple location. Error bars represent one standard deviation. (For interpretation of the references to color in this figure legend, the reader is referred to the web version of this article.)

Please cite this article in press as: Coppola AM et al. Retention of mechanical performance of polymer matrix composites above the glass transition temperature by vascular cooling. Composites: Part A (2015), http://dx.doi.org/10.1016/j.compositesa.2015.07.012

Table 6
Heat removal rate results for high temperature testing of MPC and SC specimens. Error bounds represent one standard deviation.

T (Environment) (°C)	Heat removal rate (W)							
	Mid-plane cooled (MPC) Total flow rate (mL/min)				Surface cooled (SC) Total flow rate (mL/min)			
	20	40	80	160	40	80	160	320
175	34.5 ± 1.2	36.5 ± 1.7	38.2 ± 3.7	42.8 ± 4.5	47.1 ± 1.5	50.0 ± 2.0	54.7 ± 1.4	62.2 ± 4.1
225	46.7 ± 2.3	48.5 ± 2.4	50.6 ± 4.0	56.3 ± 5.7	62.8 ± 2.4	66.7 ± 2.7	73.2 ± 1.8	80.7 ± 6.5
275	59.3 ± 2.4	61.5 ± 3.3	64.1 ± 3.8	71.0 ± 6.9	82.3 ± 2.2	85.9 ± 3.9	92.6 ± 2.8	101.3 ± 8.1
325	73.8 ± 3.7	77.5 ± 6.3	81.0 ± 7.9	91.1 ± 9.0	101.4 ± 2.7	106.3 ± 3.9	113.4 ± 1.8	123.8 ± 7.8

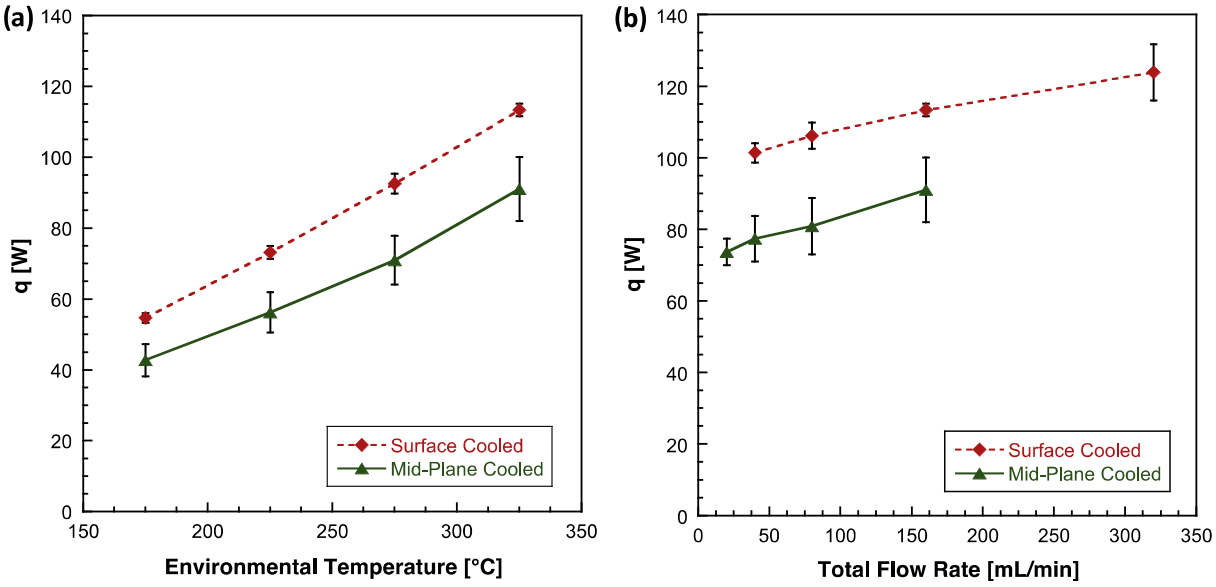

Fig. 10. Heat removal rate (q) for vascular specimens for all testing conditions. (a) Heat removal rate as a function of environmental temperature for a fixed total flow rate of 160 mL/min. (b) Heat removal rate as a function of total coolant flow rate for a fixed environmental temperature of 325 °C. Error bars represent one standard deviation. (For interpretation of the references to color in this figure legend, the reader is referred to the web version of this article.)

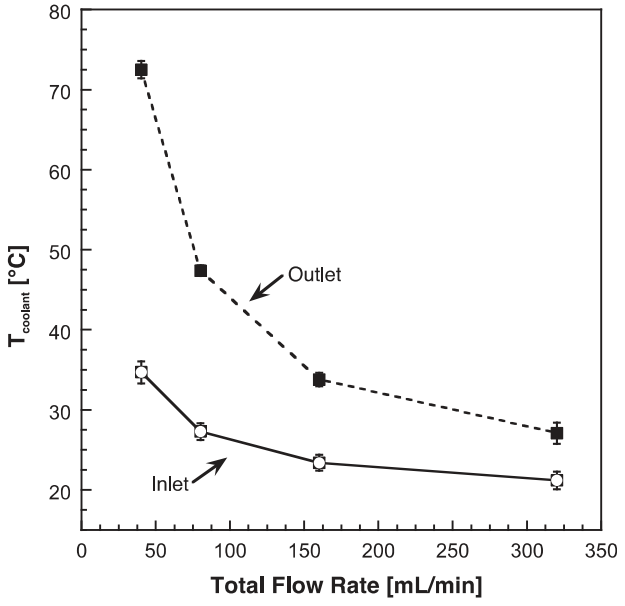

Fig. 11. Coolant temperature ($T_{coolant}$) at the inlet and outlet of the SC specimens as a function of total flow rate in a 325 °C environment. Error bar represent one standard deviation.

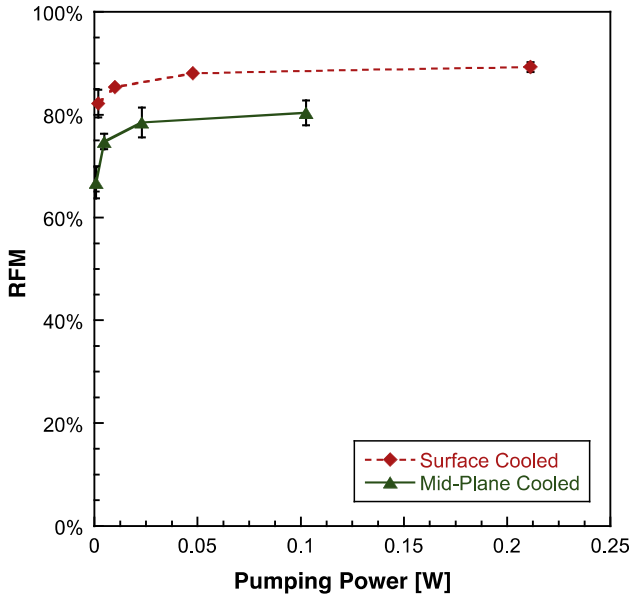

Fig. 12. RFM of actively cooled composites in a 325 °C environment as a function of total pumping power to circulate the fluid. Error bars represent one standard deviation. (For interpretation of the references to color in this figure legend, the reader is referred to the web version of this article.)

Please cite this article in press as: Coppola AM et al. Retention of mechanical performance of polymer matrix composites above the glass transition temperature by vascular cooling. Composites: Part A (2015), http://dx.doi.org/10.1016/j.compositesa.2015.07.012

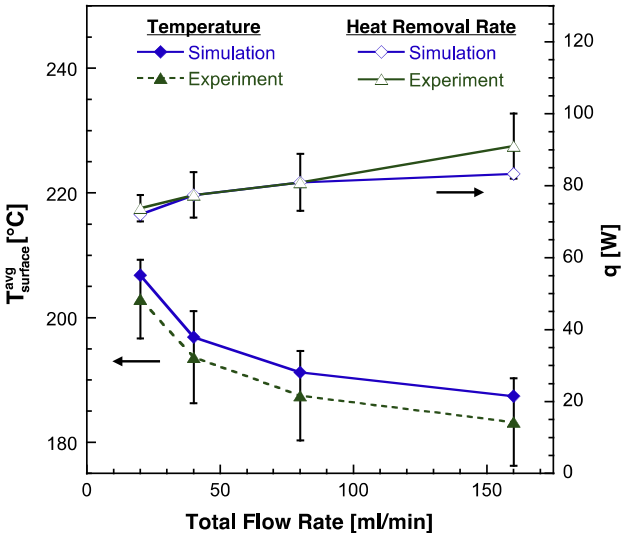

Fig. 13. Average top surface temperature ($T^{avg}_{surface}$) and heat removal rate (q) as a function of total flow rate compared for the model and experimental results at an environmental temperature of 325 °C. Results are shown for the MPC specimens. Error bars for experimental data represent one standard deviation. (For interpretation of the references to color in this figure legend, the reader is referred to the web version of this article.)

where Δp is the pressure drop through each channel. The pressure drop for each channel was evaluated from the Hagen–Poiseuille relation for laminar flow as

$$\Delta p = \frac{128\mu LQ}{\pi D^4}, \tag{4}$$

where L and D are the channel's length and diameter, respectively, and μ is the dynamic viscosity of the coolant. The temperature dependence of dynamic viscosity of water is approximated using the Seeton relation [33].

$$\mu = 0.02414 \times 10^{\frac{247.8}{T_f - 140}}, \tag{5}$$

where the viscosity is measured in centipoise and T_f (K) is the temperature of the coolant. Again, the average value of the inlet and outlet temperature was used. The Reynolds number was calculated based on channel diameter as

$$Re_D = \frac{\rho QD}{\mu A}, \tag{6}$$

where A is the channel's cross sectional area.

3.2. Characterization of control and non-cooled vascular composites

3.2.1. Room temperature testing

Control and vascular composites were tested without coolant in four-point bending according to ASTM D7264 at room temperature and flexural modulus was recorded. Eight specimens of each type were tested. Analysis of variance (ANOVA) was conducted to test for statistically significant differences and a 5% significance (*critical p-value* = 0.05) level was chosen for evaluation.

3.2.2. High temperature testing

Controls samples (no channels) were also tested at temperatures up to 325 °C for comparison to actively cooled vascular composites. Five specimens were tested at each temperature, except for the 325 °C test, where only one specimen was tested. A minimum of 10 min was allowed at each testing temperature for equilibration before beginning mechanical testing.

3.3. Characterization of neat epoxy

Dynamic mechanical analysis (DMA) was conducted according to ASTM D7028 to measure the thermomechanical behavior of the neat epoxy matrix. Specimens were cut from a neat epoxy sheet using a diamond blade wet saw. Epoxy bars measuring 2 mm × 6 mm × 35 mm were tested in three-point bending on a DMA (TA Instruments, Model RSAIII) at 1 Hz to a maximum strain of 0.1% on a 25 mm span. The temperature was ramped at 5 °C/min from 25 to 200 °C in a nitrogen environment. A nitrogen environment was selected to minimize oxidation, helping to ensure that the changes in moduli measured were due to changes in

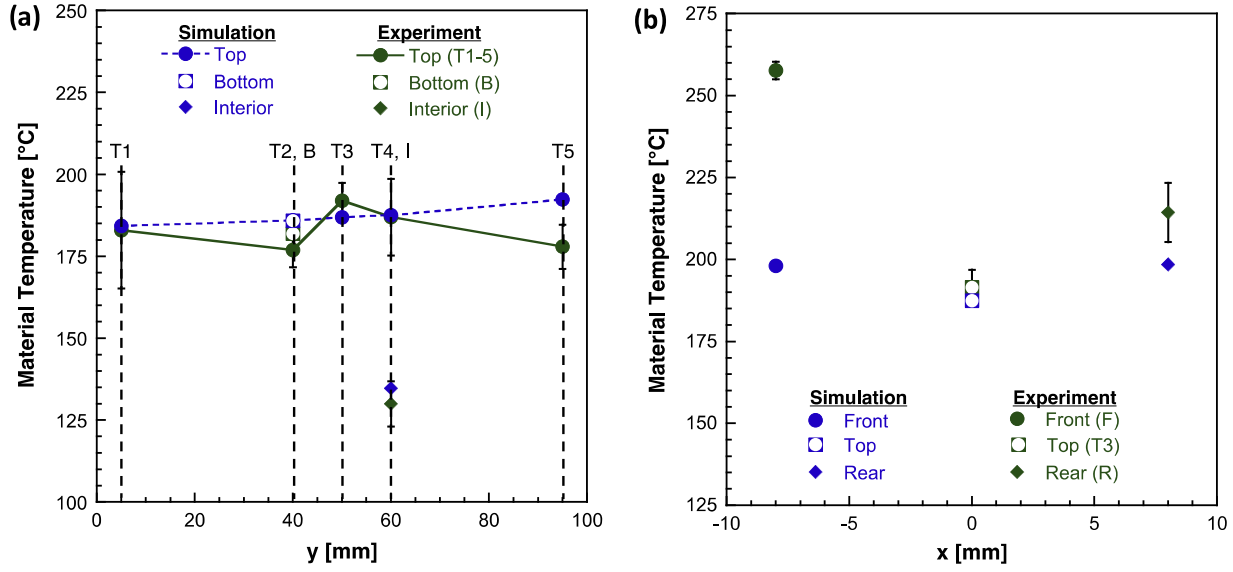

Fig. 14. Temperature distribution in actively cooled specimens compared for the model and experimental results. Temperature (a) along the $x = 0$ plane and (b) along the $y = 50$ mm plane for actively cooled composites in a 325 °C environment at a total flow rate of 160 mL/min. See Fig. 3 for detailed description of thermocouple location. Error bars for experimental data represent one standard deviation. (For interpretation of the references to color in this figure legend, the reader is referred to the web version of this article.)

Please cite this article in press as: Coppola AM et al. Retention of mechanical performance of polymer matrix composites above the glass transition temperature by vascular cooling. Composites: Part A (2015), http://dx.doi.org/10.1016/j.compositesa.2015.07.012

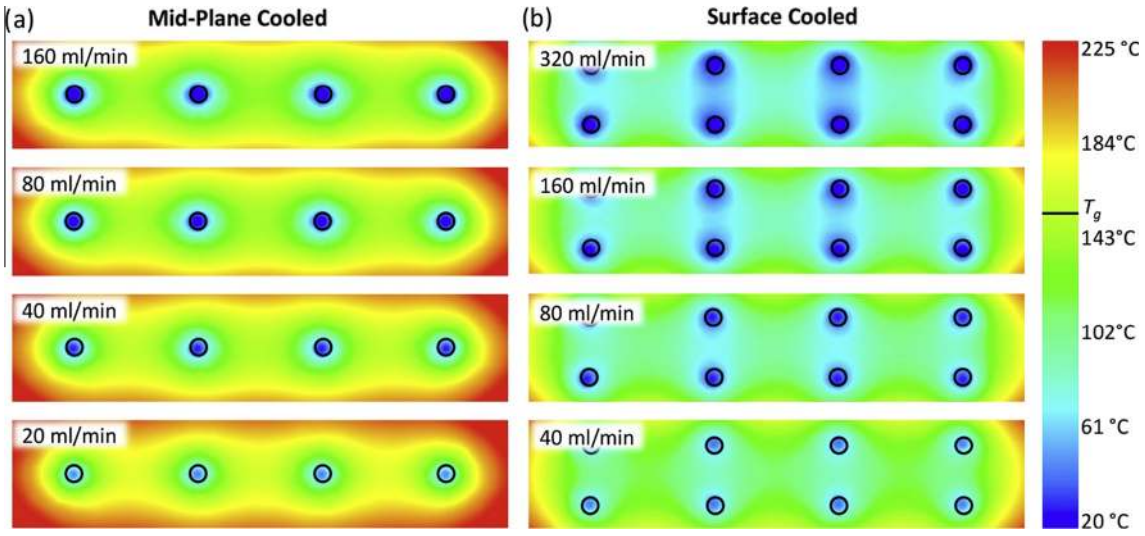

Fig. 15. Temperature profiles along the y = 50 mm plane from simulation results for the MPC and SC samples in a 325 °C environment at each value of total flow rate tested during experiments. T_g is marked on the temperature map. The edge of each channel is marked by black circles. (For interpretation of the references to color in this figure legend, the reader is referred to the web version of this article.)

temperature and not time-dependent chemical changes in the epoxy. T_g was recorded using a step transition analysis of the storage modulus (E'). Thermogravimetric analysis (TGA) was also conducted to measure thermal stability of the epoxy. Small samples of epoxy (5–10 mg) were tested by TGA (Mettler Toledo, Model TGA/DSC 1) from 25 to 600 °C at a heating rate of 10 °C/min. Tests were conducted in a mixed air/nitrogen environment, with flow rates of 35 mL/min for each. Air was included to simulate the environment experienced by the composite specimens in the environmental chamber and allow for oxidation in the degradation process. Two tests were run for both DMA and TGA to confirm repeatability.

3.4. Simulation of heat transfer and temperature fields

The thermal performance of the actively cooled composite at steady-state was simulated using a commercial computational fluid dynamics software package, ANSYS Fluent v15.0. The model included the entire microvascular composite sample, but not the coolant delivery system or the flexure fixture. Two versions of the model were created to include both the MPC and SC samples. Sample geometry was based on the experimental setup shown in Fig. 2 and the dimensions given in Section 2.2. A sample thickness of 3.5 mm was modeled. Fluid properties matched those used in the experimental analysis. Thermal conductivity of the composite was calculated using the procedure explained in Appendix A and making use of existing conductivity models for woven textiles [34,35]. The thermal conductivities of the composite were calculated both in-plane $k_x = k_y = 0.609$ W/m K and out-of-plane $k_z = 0.450$ W/m K. The thermal conductivity of the water was taken as $k_w = 0.600$ W/m K.

As in the experiment, water was distributed evenly through each of the channels along the y-direction. Fluid flow rate and environmental temperature were chosen to match the values used for the experiment. Inlet water temperature was set to the value measured during the experiment to eliminate the need to model the heating of the fluid in the coolant delivery system. Heat was provided to the specimens by a combined uniform convection and radiative heating on all surfaces of the sample. The convection coefficient was chosen to best fit both the heat removal rate and temperature field measured during the experiment. In this way, the convection coefficient took into account both sample heating from the air and from contact with the fixture. A value of $h = 130$ W/m^2 K was used for all tests. The emissivity of the sample surface was set to 0.95, based on the emissivity of the black paint applied to all samples.

A conforming, hexahedral finite volume mesh was generated to simulate the MPC and SC samples using ANSYS Meshing v15.0. The MPC mesh contained 91,200 fluid elements and 159,000 solid elements and the SC mesh contained 182,550 fluid elements and 229,950 solid elements. More elements were used in the SC mesh to provide sufficient resolution of the mesh around the additional channels. Temperature at steady state was not appreciably changed by using meshes with either more and less elements (see Table 2 for the MPC model). Simulations were performed in ANSYS Fluent using the SIMPLE pressure–velocity coupling scheme, Green-Gauss node-based gradient discretization, second-order pressure discretization, third-order MUSCL momentum discretization, and third-order MUSCL energy discretization. The model solved for the conversation of mass, momentum and energy for an incompressible Newtonian fluid with laminar flow. The convergence criteria were for velocity and continuity residuals to reach 10^{-4} and energy residuals to reach 10^{-8}.

4. Results and discussion

4.1. Effect of vascularization on flexural modulus at room temperature

Room temperature flexural test results are presented in Table 3. No statistically significant difference in flexural modulus was found (p-value = 0.0503 from ANOVA). No appreciable difference in average modulus was measured between the non-vascular controls and MPC specimens, as expected. A slight reduction is reported for SC specimens although it is well within experimental scatter.

4.2. Thermomechanical behavior of neat epoxy

DMA testing reveals a gradual reduction in storage modulus below the T_g of 152 °C followed by a drop of almost two orders of magnitude above T_g (Fig. 5a). The peak in tan(δ) is 160 °C. Mass loss was detected by TGA as early as 200 °C and reached 3 wt% by 325 °C (Fig. 5b). A sharp drop in mass is noted at roughly 360 °C.

Please cite this article in press as: Coppola AM et al. Retention of mechanical performance of polymer matrix composites above the glass transition temperature by vascular cooling. Composites: Part A (2015), http://dx.doi.org/10.1016/j.compositesa.2015.07.012

4.3. Thermomechanical behavior of actively cooled composites

Active cooling of composites leads to vastly improved mechanical performance at high temperature (Fig. 6 and Table 4). For SC specimens nearly 90% RFM is achieved at 325 °C environmental temperature with a total coolant flow rate of 160 mL/min. In stark contrast, control specimens possess no structural capacity at the same temperature and show a sharp drop in flexural modulus when the environmental temperature approaches the T_g of the matrix. Actively cooled composites have a small change in properties near T_g and only a modest decrease in flexural modulus over the entire range of temperatures tested.

The effect of vascular architecture on RFM is also revealed in Fig. 6. SC specimens retained higher flexural modulus than MPC specimens at the same total coolant flow rate. Given that the SC architecture distributed the coolant closer to the surface, this configuration is more effective at cooling the specimen (see Fig. 8) and results in higher retention of flexural modulus.

The effect of flow rate on RFM is presented in Fig. 7. In both SC and MPC architectures increasing total coolant flow rate leads to higher retained modulus. Importantly, the SC architecture is more effective compared to MPC at all flow rates tested. Even the lowest flow rate tested for the SC architecture (40 mL/min) outperforms the MPC architecture at the highest flow rate (160 mL/min). These results emphasize the crucial role that the vascular architecture plays in maximizing cooling effectiveness. Increasing flow rate eventually becomes less effective in either architecture as the coolant traverses the channels too quickly to extract additional heat (see Fig. 11).

4.4. Temperature of actively cooled composites

Temperature of the actively cooled composites is influenced by channel architecture, coolant flow rate, and environmental temperature. The average top surface temperature for all test conditions is reported in Table 5 and plotted in Fig. 8. Under maximum cooling (SC at 320 mL/min), the top surface temperature was reduced to 151 °C (*ca.* 40% of environmental temperature) in the 325 °C environment. The SC architecture cooled more effectively than the MPC architecture at all environmental temperatures and for all flow rates. For both architectures, the relation between surface temperature and flow rate is non-linear, with the surface temperature gradually leveling off as flow rate is increased.

Fig. 9 shows the temperature distribution in a 325 °C environment for both MPC and SC specimens at 160 mL/min flow rate. The top surface temperature (T1-5) shows no evidence of the increase in coolant temperature along the *y*-direction (*ca.* 10 °C rise, see Fig. 11). Non-uniform heating from variations in the airflow currents and contact with the fixtures may have obscured the effect of increasing coolant temperature on surface temperature. The bottom thermocouple (B) measured temperatures nearly identical to the corresponding top thermocouple (T2) for both MPC and SC specimens. The internal thermocouple (I) measured a lower temperature than the corresponding top surface thermocouple (T4), indicating non-uniform temperature through the thickness. Interestingly, the surface temperature of both MPC and SC specimens was at or above T_g in the 325 °C environment. However, internal temperature of the SC specimens was reduced to just 96 ± 7 °C in the 325 °C environment under 160 mL/min total flow rate. The temperature of the MPC specimens in the same location was only reduced to 130 ± 7 °C, much closer to T_g. The highest temperatures for both architectures were observed at the front and rear edges of the specimen due to limited cooling at these boundaries. The airflow direction (front to back) led to a higher temperature on the front edge ($x = -8$ mm) than the rear edge ($x = 8$ mm).

4.5. Heat removal rate by the active cooling network

The total heat removal rates for all experiments are given in Table 6. Active cooling at maximum flow rate for SC specimens removed 120 W of heat in a 325 °C environment. In general, heat removal rates increased linearly as a function of environmental temperature and flow rate (Fig. 10). SC specimens removed more heat than MPC specimens for all flow rates tested and environmental temperatures. Heat removal rate depended explicitly on the temperature differential of the coolant from inlet to outlet. Fig. 11 shows the temperature of the coolant at the inlet and the outlet as a function of the total flow rate in a SC specimen in a 325 °C environment. Both inlet and outlet temperatures converged at higher flow rates, although heat removal rate continued to increase linearly for the flow rate range tested (Fig. 10b).

4.6. Pumping power considerations on active cooling

Active cooling effectiveness was shown to depend on both architecture and flow rate. Increasing the total flow rate and dispersing the flow through more channels placed near the surface improved active cooling effectiveness, but with the penalty of increased pumping power. Fig. 12 shows the RFM as a function of total pumping power. While increased pumping power provided modest benefits initially, RFM was nearly constant at high pumping powers. This trend was more dramatic than when comparing RFM to flow rate because pumping power increases with the square of the flow rate. Selection of an appropriate flow rate based on the total heat load and target temperature is important for minimizing wasted energy as a result of excessive pumping power. SC specimens had higher RFM than MPC specimens with respect to pumping power, indicating that dispersing the flow through more channels placed near the surface was more energy efficient.

4.7. Experimental results vs. simulation

Simulation results are compared to experimental data in Figs. 13 and 14, showing good agreement. Fig. 13 compares the average top surface temperature and heat removal rate as a function of total flow rate through the mid-plane cooled specimen. All simulation results fall within the error bars for the experiment. Similar trends were found for the SC simulation. Fig. 14 compares the point-by-point temperature distribution throughout the MPC composite at an environmental temperature of 325 °C and total flow rate of 160 mL/min. Along the $x = 0$ plane, most points fall within the experimental error. The simulation results show that the temperature should steadily increase along the top surface from inlet to outlet as the coolant temperature increases. This trend was not observed during the experiment however and we attribute this to variations in air currents within the convective oven and contact with the sample loading fixture. Along the $y = 50$ mm plane, good agreement occurs for the top surface, but the front side shows significant differences. Again, this is likely due to differences in convection over the sample surface within the oven. These results indicate that the convective coefficient is significantly higher on the front edge of the sample. Nevertheless, the overall thermomechanical behavior and main conclusions are unaffected.

4.8. Through-thickness temperature profiles

The cross-sectional temperature profiles from simulation are shown in Fig. 15 for the MPC and SC samples for an environmental temperature of 325 °C and at each value of total flow rate. Local to each channel the temperature is reduced significantly and the

Please cite this article in press as: Coppola AM et al. Retention of mechanical performance of polymer matrix composites above the glass transition temperature by vascular cooling. Composites: Part A (2015), http://dx.doi.org/10.1016/j.compositesa.2015.07.012

center of each specimen is significantly cooler than the outer surfaces. Placement of the channels near the surface in the SC sample results in greatly reduced temperature throughout the thickness relative to the MPC sample. Increased flow rate decreases temperature throughout the cross section and, importantly, reduces the portion of the specimen above T_g. However, even at the lowest flow rate for the MPC case, a significant portion of the specimen is still below T_g, providing material with sufficient modulus to sustain the flexural load.

5. Conclusions

In this study, the thermomechanical behavior of actively cooled vascularized composites was examined during a four-point bending test in a convectively heated chamber. Structural performance of actively cooled specimens was dramatically improved compared to non-cooled controls. Actively cooled specimens retained up to 90% of their room temperature flexural modulus at 325 °C. In contrast, non-cooled control specimens showed a sharp reduction in flexural modulus above glass transition temperature and complete loss of structural capability at 325 °C. Improved structural performance in actively cooled specimens resulted from heat removal and the corresponding decrease in material temperature. Thermal testing indicated non-uniform temperature in actively cooled specimens. Surface temperature rose above T_g for both architectures in the 325 °C environment, while the internal temperature was maintained below T_g. However, even in these cases only modest reductions in the structural performance occurred. Flexural modulus increased and composite temperature decreased non-linearly as a function of flow rate, with the greatest performance improvement at low flow rates. Heat removal rate also increased with flow rate but showed a more linear trend. Surface cooled composites outperformed mid-plane cooled composites throughout testing, even when pumping power was taken into account, indicating the importance of channel architecture on cooling performance.

Simulations of the heat transfer showed good agreement with experimental measurements for both temperature and heat removal rates. Temperature profiles of the actively cooled specimens from simulation confirmed the presence of a temperature gradient, with the highest temperatures on the surface and reduced temperature near the channel walls. In all cases, a portion of the actively cooled specimens was maintained below T_g, allowing for the specimen to retain mechanical performance (flexural modulus) in comparison to samples that were not cooled.

Acknowledgments

The authors would like to acknowledge the financial support by the Air Force Office of Scientific Research as part of a Multidisciplinary University Research Initiative, Award No. FA9550-09-1-0686, *Synthesis, Characterization and Prognostic Modeling of Functionally Graded Hybrid Composites for Extreme Environments*. Financial support was also provided by the National Science Foundation Graduate Research Fellowship under Grant No. DGE 11-44245. The authors would also like to thank Stephen Pety for his assistance with developing the Fluent Simulation and Greg Milner of the UIUC Talbot Lab machine shop for assistance with sample preparation.

Appendix A

In-plane and transverse thermal conductivities of the three-dimensional woven glass fiber/epoxy composite were calculated using the following procedure. The textile shown in Fig. 1 is modeled as a $[90/0]_s$ composite, to take into account the difference in tow spacing that leads to nearly equivalent fiber content in the warp and weft directions. Based on this assumption, the in-plane thermal conductivity is

$$k_x = k_y = (1/2)k_l + (1/2)k_t, \tag{7}$$

where k_l is the thermal conductivity of a unidirectional composite in the direction longitudinal to the fibers and k_t is the thermal conductivity transverse to the fibers. The out-of-plane thermal conductivity is

$$k_z = k_t. \tag{8}$$

The longitudinal thermal conductivity is then calculated [34] as

$$k_l = k_f V_f + k_m(1 - V_m), \tag{9}$$

and the transverse thermal conductivity is calculated [35] as

$$k_t = k_m \frac{k_m + k_f + V_f(k_f - k_m)}{k_m + k_f - V_f(k_f - k_m)}. \tag{10}$$

Here k_m and k_f are the thermal conductivities of the matrix and fiber, respectively. The matrix conductivity is 0.23 W/m K and the fiber conductivity is 1.45 W/m K [16]. V_f is the fiber volume fraction, which was assumed uniform throughout the composite and equal to 0.445. The resulting in-plane thermal conductivity is $k_x = k_y = 0.609$ W/m K and out-of-plane is $k_z = 0.450$ W/m K.

References

[1] Meese EA, Nørstrud H. Simulation of convective heat flux and heat penetration for a spacecraft at re-entry. Aerosp Sci Technol 2002;6(3):185–94.
[2] Hengeveld D, Mathison M, Braun J, Groll E, Williams A. Review of modern spacecraft thermal control technologies. HVACR Res 2010;16(2):189–220.
[3] Meetham GW. High-temperature materials-a general review. J Mater Sci 1991;26:853–60.
[4] Sonsino C, Moosbrugger E. Fatigue design of highly loaded short-glass-fibre reinforced polyamide parts in engine compartments. Int J Fatigue 2008;30(7):1279–88.
[5] Johnson RW, Evans JL, Jacobsen P, Thompson JRR, Christopher M. The changing automotive environment: high-temperature electronics. IEEE Trans Electron Packag Manuf 2004;27(3):164–76.
[6] Boyd J. BMI composites. In: Donaldson SL, Micracle DB, editors. ASM handbook volume 21: composites. Materials Park, OH: ASM International; 2001. p. 100–4.
[7] Park J, Li X. Effect of flow and temperature distribution on the performance of a PEM fuel cell stack. J Power Sources 2006;162(1):444–59.
[8] Rao Z, Wang S. A review of power battery thermal energy management. Renew Sustain Energy Rev 2011;15(9):4554–71.
[9] Sabbah R, Kizilel R, Selman JR, Al-Hallaj S. Active (air-cooled) vs. passive (phase change material) thermal management of high power lithium-ion packs: Limitation of temperature rise and uniformity of temperature distribution. J Power Sources 2008;182(2):630–8.
[10] Mouritz AP, Feih S, Kandare E, Mathys Z, Gibson AG, Des Jardin PE, et al. Review of fire structural modelling of polymer composites. Composites Part A 2009;40(12):1800–14.
[11] Chowdhury EU, Eedson R, Bisby LA, Green MF, Benichou N. Mechanical characterization of fibre reinforced polymers materials at high temperature. Fire Technol 2009;47(4):1063–80.
[12] Kandare E, Kandola BK, Myler P, Edwards G. Thermo-mechanical responses of fiber-reinforced epoxy composites exposed to high temperature environments. Part I: experimental data acquisition. J Compos Mater 2010;44(26):3093–114.
[13] Kandola BK, Horrocks AR, Myler P, Blair D. Mechanical performance of heat/fire damaged novel flame retardant glass-reinforced epoxy composites. Composites Part A 2003;34(9):863–73.
[14] Kozola BD, Shipton LA, Natrajan VK, Christensen KT, White SR. Characterization of active cooling and flow distribution in microvascular polymers. J Intell Mater Syst Struct 2010;21(12):1147–56.
[15] Soghrati S, Thakre PR, White SR, Sottos NR, Geubelle PH. Computational modeling and design of actively-cooled microvascular materials. Int J Heat Mass Transf 2012;55(19–20):5309–21.
[16] Soghrati S, Najafi AR, Lin JH, Hughes KM, White SR, Sottos NR, et al. Computational analysis of actively-cooled 3D woven microvascular composites using a stabilized interface-enriched generalized finite element method. Int J Heat Mass Transf 2013;65:153–64.
[17] Norris CJ, Meadway GJ, O'Sullivan MJ, Bond IP, Trask RS. Self-healing fibre reinforced composites via a bioinspired vasculature. Adv Funct Mater 2011;21(19):3624–33.

Please cite this article in press as: Coppola AM et al. Retention of mechanical performance of polymer matrix composites above the glass transition temperature by vascular cooling. Composites: Part A (2015), http://dx.doi.org/10.1016/j.compositesa.2015.07.012

[18] Norris CJ, Bond IP, Trask RS. The role of embedded bioinspired vasculature on damage formation in self-healing carbon fibre reinforced composites. Composites Part A 2011;42(6):639–48.
[19] Norris CJ, Bond IP, Trask RS. Interactions between propagating cracks and bioinspired self-healing vascules embedded in glass fibre reinforced composites. Compos Sci Technol 2011;71(6):847–53.
[20] Wu AS, Coppola AM, Sinnott MJ, Chou T-W, Thostenson ET, Byun J-H, et al. Sensing of damage and healing in three-dimensional braided composites with vascular channels. Compos Sci Technol 2012;72(13):1618–26.
[21] Huang C-Y, Trask RS, Bond IP. Characterization and analysis of carbon fibre-reinforced polymer composite laminates with embedded circular vasculature. J R Soc Interface 2010;7(49):1229–41.
[22] Williams G, Trask R, Bond I. A self-healing carbon fibre reinforced polymer for aerospace applications. Composites Part A 2007;38(6):1525–32.
[23] Bleay S, Loader C, Hawyes V, Humberstone L, Curtis P. A smart repair system for polymer matrix composites. Composites Part A 2001;32(12):1767–76.
[24] Pang JWC, Bond IP. A hollow fibre reinforced polymer composite encompassing self-healing and enhanced damage visibility. Compos Sci Technol 2005;65(11–12):1791–9.
[25] Phillips DM, Ryan Pierce M, Baur JW. Mechanical and thermal analysis of microvascular networks in structural composite panels. Composites Part A 2011;42(11):1609–19.
[26] Kousourakis A, Bannister MK, Mouritz AP. Tensile and compressive properties of polymer laminates containing internal sensor cavities. Composites Part A 2008;39(9):1394–403.
[27] Kousourakis A, Mouritz AP. The effect of self-healing hollow fibres on the mechanical properties of polymer composites. Smart Mater Struct 2010;19(8):085021.
[28] McCombe GP, Rouse J, Trask RS, Withers PJ, Bond IP. X-ray damage characterization in self-healing fibre reinforced polymers. Composites Part A 2012;43(4):613–20.
[29] Dong H, Esser-Kahn AP, Thakre PR, Patrick JF, Sottos NR, White SR, et al. Chemical treatment of poly(lactic acid) fibers to enhance the rate of thermal depolymerization. ACS Appl Mater Interfaces 2012;4(2):503–9.
[30] Esser-Kahn AP, Thakre PR, Dong H, Patrick JF, Vlasko-Vlasov VK, Sottos NR, et al. Three-dimensional microvascular fiber-reinforced composites. Adv Mater 2011;23(32):3654–8.
[31] Coppola AM, Thakre PR, Sottos NR, White SR. Tensile properties and damage evolution in vascular 3D woven glass/epoxy composites. Composites Part A 2014;59:9–17.
[32] Phillips DM, Baur JW. A microvascular method for thermal activation and deactivation of shape memory polymers. J Intell Mater Syst Struct 2013;24(10):1233–44.
[33] Seeton CJ. Viscosity–temperature correlation for liquids. Tribol Lett 2006;22(1):67–78.
[34] Ning Q-G, Chou T-W. Closed-form solutions of the in-plane effective thermal conductivities of woven-fabric composites. Compos Sci Technol 1995;55(1):41–8.
[35] Rolfes R. Transverse thermal conductivity of CFRP laminates: a numerical and experimental validation of approximation formulae. Compos Sci Technol 1995;54(1):45–54.

Please cite this article in press as: Coppola AM et al. Retention of mechanical performance of polymer matrix composites above the glass transition temperature by vascular cooling. Composites: Part A (2015), http://dx.doi.org/10.1016/j.compositesa.2015.07.012